JOINT EUROPEAN TORUS JET

JET–P(84)02

R.J. Bickerton

Physics Performance of the Joint European Torus (JET)

Physics Performance of the Joint European Torus (JET)

R.J. Bickerton

JET-Joint Undertaking, Culham Science Centre, OX14 3DB, Abingdon, UK

Preprint of Paper to be submitted for publication in
Plasma Physics and Controlled Fusion

PHYSICS PERFORMANCE OF THE JOINT EUROPEAN TORUS

R J Bickerton

JET Joint Undertaking, Abingdon, Oxfordshire OX14 3EA, England

ABSTRACT

JET has been operating for one year. The diagnostic capability has been progressively increased from the barely adequate initial level to the point where physics data on the internal plasma processes is available. The plasma current has been taken up to just over 3 MA with flat-top times of several seconds. Central electron temperatures are in the range 1-3 keV, mean electron densities (n) from $0.1 - 2.5 \times 10^{19} m^{-3}$ and the derived global energy confinement τ_E reaches $0.35_S \pm 30\%$. The radiation loss is substantial, ranging from 60 - 100% of the input power. The contamination of the plasma is high, giving typical values of $Z_{eff} \sim 5$, limiting the maximum density, giving higher temperatures and lower $\langle n\tau_E \rangle$ products than expected. Experiments and machine changes are in hand to overcome this problem.

INTRODUCTION

The Joint European Torus (JET) is a large tokamak designed and built with the ultimate aim of reaching near fusion-reactor plasma conditions in a $\sim$5 MA discharge in deuterium-tritium mixture. To reach this goal substantial additional heating by neutral beam (10 MW) and radio frequency (15 MW) methods is planned. This paper reports the preliminary results obtained with only the ohmic heating due to the passage of high currents through the gas. The main design parameters of the JET apparatus are listed in Table 1. The apparatus has been described in more detail by Rebut and Green (1983).

MACHINE STATE

All discharges in the first year of operation have been in hydrogen gas. The vacuum vessel is baked to 270°C and the connecting ports to 210°C for $\sim$2 days after a vacuum opening. After pump-down the system is then glow discharge cleaned for typically 72 hours. The resulting base pressure is typically $\sim 10^{-7}$mbar at 250°C.

In all the experiments described four carbon limiters are used, placed $\sim$20 cm in from the vacuum vessel wall on the equatorial plane, large major radius side. Each limiter measures 0.8 m in the vertical direction and 0.4 m in the horizontal (toroidal) direction. The limiters are slightly curved in the toroidal direction to accommodate scrape-off plasmas with thicknesses up to 3 cm. The results reported here were all obtained with the vacuum vessel at the elevated temperature of 250°C. Compared with earlier operation with room temperature walls this seems to give a faster rate of density decay at the end of the pulse as the plasma current is ramped down, and therefore fewer disruptive instabilities. This contention has not yet been proved in definitive experiments.

DIAGNOSTICS

The diagnostics on the machine have been progressively increased in the year of operation from June 1983 to June 1984. The data reported here was obtained with the following systems:-

1. Magnetic Measurements

Each octant of the machine is equipped with 18 internal poloidal field pick-up coils; there are several volts/turn loops at different poloidal positions on the vacuum vessel, and many flux loops on the surface of the vessel to measure the normal components of flux. From these measurements it is possible to measure the plasma current Ip(t), the voltage per turn V(t), the plasma position, the shape of the flux surfaces, the plasma inductance and poloidal beta. The direct measurements are accurate to ± 2%.

2. Interferometer

A single channel 2 mm microwave interferometer measures $\int n_e d\ell$ along a single vertical chord at the major radius $R = 3.14$ m. The line average density $\bar{n} = \frac{\int n_e d\ell}{\int d\ell}$ is obtained using the value of the $\int d\ell$ from the outer flux surface as derived from magnetic measurements.

3. Microwave-reflectometer

The shape of the density profile has been estimated using a microwave reflectometer. This uses a fixed frequency ($\sim$30 GHz) on a given pulse and essentially measures interferometrically the motion on the equatorial plane of the radius R at which the density is equal to the critical value for reflection ($n_e \sim 10^{19} m^{-3}$). If the shape of the density profile is assumed to be unchanged as the density rises then $n_e(R)$ can be deduced.

4. Electron-cyclotron Emission

The electron temperature profile is deduced by analysis of the E-mode emission at the second harmonic of the electron cyclotron frequency. The measurements are made along a chord in the equatorial plane and are limited by harmonic overlap effects to major radii >2.8 m. The temperature determination depends on the absolute calibration of the system which has been done by a variety of methods to an accuracy of ± 20%.

5. Visible Light

Visible light has been analysed using a close-coupled spectrometer and also a variety of filters and spectrometers looking at light transmitted $\sim$100m through optical fibres. Some lines of sight look at the surface of the carbon limiters and some at the vessel wall. The measurements enable the impurity elements to be identified and the injection rates of impurities and hydrogen from various locations to be estimated.

One line of sight looks vertically through the plasma into an opposite port. The intensity at the wavelength 523 nm is measured. There is no detectable line emission in this region and the emission is assumed to be due to bremsstrahlung radiation. The intensity is then proportional to $\frac{n_e^2 Z_{eff}}{T_e^{\frac{1}{2}}}$ integrated along the line of sight, where $Z_{eff} = \frac{\Sigma n_i Z_i^2}{n_e}$. Because of the strong dependence on density the mean value of Z_{eff} deduced in this way is weighted towards the centre of the plasma.

6. Vacuum Ultra-Violet Spectrometer

For the later discharges reported here a broad-band (10 - 170 nm) spectrometer was operational. This permits identification of impurity elements and their concentrations deeper in the plasma than is possible with the visible light observations.

7. Soft X-Ray Diodes

Four soft X-ray diodes have been used to view the plasma along a chord in the equatorial plane through filters of varying thickness. These measurements show that for all the discharges reported here and starting early in the pulse there is characteristic sawtooth activity corresponding to the safety factor $q \left(= \frac{r^2}{2R} \frac{B\phi}{I_p(r)}\right)$ in the centre falling to values close to unity. The sawtooth period is typically 30 - 50 ms.

8. Limiter-viewing

Infra-red cameras have been used to inter alia measure the surface temperature of at least one carbon limiter. The measurements show local heating to $\sim$800°C in typical cases. From the location of the heated zones it is deduced that the scrape-off plasma in the shadow of the limiters has a thickness of $\sim$15 mm.

9. Bolometry

At one toroidal location there are three bolometer cameras viewing the plasma along 32 chords in the meridional plane. These bolometers are sensitive to radiation and to fluxes of charge-

exchange neutral particles. These fluxes are estimated to be small compared with the contribution from radiation. Consequently the camera measurements can be 'Abel-inverted' to give the local radiated power P_{RAD} as a function of R, z and t. Single bolometers placed in different toroidal locations confirm the toroidal symmetry of radiated power.

PLASMA RESULTS

The results reported here were obtained with toroidal field strengths in the range 1.6 - 2.6 T and plasma currents 1 - 3 MA. The plasma position is controlled by two feedback systems, one controlling the horizontal position through the applied vertical magnetic field (B_Z) and the other maintaining up-down symmetry of the plasma by application of radial magnetic field (B_R). The elongation of the plasma, i.e. the ratio of the vertical plasma 'radius' b, to the horizontal 'radius' a, is not actively controlled. It is partly predetermined by the turns ratios used in the poloidal field coils and strongly influenced by the current distribution within the plasma, so that the flatter the distribution, the greater is the elongation b/a .

Figure 1 shows the plasma current, loop voltage and density for a typical pulse in the 1983 campaign. The loop voltage on the flat top of the current pulse is usually in the range 0.8 - 1.2V on JET. Figure 2 shows the outer bounding magnetic surface versus time for this discharge. It shows the elongation $\sim$ 1.1 and the expanding aperture used in the current rise phase of all pulses reported here with the aim of minimising skin effects. Figure 3 shows the flat-top values of plasma current and density for the discharges reported here. The data is divided into three groups - near-circular discharges ($b/a < 1.2$) for 1983, the same for 1984, and elliptic discharges ($b/a > 1.3$) for 1984. Figure 4 shows the corresponding values for Z_{eff} versus density classified in the same way. It is clear that Z_{eff} decreases rapidly as the density increases and that the impurity contamination is greater in 1984 than in 1983. This is reflected in other data; for example the electron temperatures are consistently higher in the 1984 data discussed here than in 1983.

Discharges are found to disrupt at any phase of the discharge if the density exceeds a critical value (n_D) proportional to the current density where

$$n_D = 6 \times 10^{19} \frac{I_p(MA)}{A(m^2)} \quad m^{-3} \qquad (1)$$

where A is the cross-sectional area of the discharge. The disruptive behaviour is of the typical tokamak type - first a rapid loss of thermal energy accompanied by a flattening of the current profile followed by a fast decay of the current to zero, e.g. 2.7 MA to zero in 30 ms in an extreme JET case.

Figures 5 - 9 show data from one elliptic discharge ($b/a = 1.5$). The toroidal magnetic field strength is 2.05 T, $Z_{eff} = 5.6$, and the Shafranov safety factor q_ψ at the plasma boundary is 3.6 at full current. Figure 5 shows the plasma current, peak and area-weighted electron temperatures from electron cyclotron emission and electron density versus time. Note the early rise of the central electron temperature and the slower rise of the average value, indicating a broadening of the profile as the $q = 1$ region expands. Figure 6 shows the flux surfaces at 7.2 s into the pulse. The discharge is well-centred and up-down symmetric. The derived value of β_p is 0.12. Figure 7 shows the density profile derived from the reflectometer measurements. The profile is approximately parabolic with the extrapolated central value $\sim$50% higher than the line average density. Figure 8 shows the electron temperature profile evolution during the flat-top of the discharge, i.e. at 4 and 7 seconds. Within the errors the profiles are the same. Figure 9 shows the profiles of ohmic power input and radiated power at $t = 7$ s. The ohmic power is obtained from $\bar{E}.\bar{j}$ where j is from the magnetic measurements and $\bar{E}$ is from the loop voltage appropriately corrected for measured inductive changes during the flat-top. For this case $\sim$70% of the total power input is radiated. For the discharges reported here the ratio $\int P_{RAD}\, dV / \int P_\Omega\, dV$ ranges from 0.6 - 1.0. From Fig. 9 it is evident that in the core of the plasma only $\sim$30% of the input power is radiated. This is again typical of the data set.

The global energy confinement time is defined as

$$\tau_\varepsilon = \frac{W_e + W_i}{\int P_\Omega dV - \frac{d}{dt}(W_e + W_i)} \qquad (2)$$

where W_e and W_i are the total electron and ion energy contents in the plasma respectively. Calculations are carried out towards the end of the flat-top phase so that $\frac{d}{dt}(W_e+W_i)$ is normally negligible. The electron content has been calculated using the temperature profiles from the electron cyclotron emission measurement and assuming the density to have the constant line-average value. Incorporating the measured profile would have a negligible effect essentially because of the similarity in temperature and density profiles coupled with the overall constraint of the measured line integral. The ion temperature is assumed to be 0.9 T_e. The ratio of ion to electron densities is derived from the expression:-

$$\frac{n_i}{n_e} = \frac{\bar{Z}_i + 1 - Z_{eff}}{\bar{Z}_i} \qquad (3)$$

where $\bar{Z}_i$ is the mean charge of the impurity ions. $\bar{Z}i$ is taken to be 12 as representative of a mixture of light impurities such as oxygen, and metals such as nickel. For a typical case such as the pulse featured in Figures 5 - 9, $W_i \sim 0.5 - 0.6\ W_e$. Figure 10 shows the resulting global energy confinement times plotted versus density. Closer examination of the data shows the confinement to increase with q_ψ; Figure 11 shows such a representation in which the spread of the data is reduced by plotting τ_ε vs $\bar{n}_e\ q_\psi^{0.8}$. The error in the confinement time determination which depends strongly on the temperature measurements is estimated to be ± 30%. In these circumstances it is clear that the indices in the above scaling expression are not precisely determined. The JET results are consistent with the scaling $\tau_\varepsilon = 7\times10^{-22}\ nR^2\ a\ q^{0.8}$ found by analysis of PLT and TFTR data. (Hawryluk et al). For constant n, B and I_p increasing ellipticity improves the confinement time, essentially through the effect on q_ψ. However from (1) the maximum plasma density is proportional to the current density, i.e. $n \propto B_\phi/R_q$. It follows that the <u>maximum</u> confinement time is determined primarily by the ratio B_ϕ/R and is not sensitive to elongation. This is manifest in the data where the same maximum confinement time is found for near circular and elongated plasmas.

The global confinement time obtained for the pulse featured earlier is 0.32s. Taking the plasma parameters on axis we can calculate a central confinement time $\tau_\varepsilon(0)$, defined as

$$\tau_\varepsilon(0) = \frac{3}{2}\ \frac{n(0)\ T_e(0)}{P_\Omega(0)}\ \left(1 + \frac{W_i}{W_e}\right) \qquad (4)$$

For the featured pulse $\tau_\varepsilon(0) = 0.29$s, i.e. essentially the same as the global value. Consequently the value of $(n(0)\ \tau_\varepsilon(0))$ achieved in the centre of the plasma is approximately $8 \times 10^{18} m^{-3}s$. This is representative of the best pulses in the data set.

The spectroscopic observations show the plasmas to be contaminated with carbon, oxygen, chlorine, chromium, nickel and molybdenum. Measurements viewing the limiter and the wall show the injection of metals to be taking place primarily at the limiter. Surface analysis of carbon tiles from the limiter show significant surface coverage with nickel, chromium and molybdenum. The nickel and chromium are essentially from the Inconel walls and are deposited on the limiters during glow discharge cleaning and during disruptions. The molybdenum is most probably the result of the manufacturing process used to make and treat the tiles. Chlorine is believed to come from the detergent used in washing the torus.

The spectroscopic and bolometric observations are consistent with a central plasma contamination of approximately 0.2 to 0.3% of metals such as nickel together with approximately 3% of light impurities such as oxygen.

Observations of the H_α light show that the hydrogen recycling is taking place predominantly at the limiters, with the wall contribution only becoming signficant for elongated plasmas.

Since these experiments, two new diagnostic systems have been brought into operation, and have given important new data. In the first, Thomson scattering measurements have confirmed the electron cyclotron emission values for the central electron temperature. This implies, although it does not prove, that the values reported here are correct with a higher precision than that quoted. The second system is a single channel of the neutral particle analyser which shows the central ion temperature, uncorrected for neutral opacity, to be typically 70% rather than 90% of the central electron temperature. If 0.7 rather than 0.9 is used uniformly across the radius as the ratio $T_{i/Te}$ it reduces the confinement times quoted here by about 8%.

CONCLUSIONS

In the first year of operation JET has reached currents of 3 MA, electron temperatures up to 3 keV, electron densities up to $2.5 \times 10^{19} m^{-3}$ and q_ψ down to 2.6. The global confinement times (τ_E) reached 0.35s and are consistent with the scaling obtained from PLT and TFTR in which $\tau_E = 7 \times 10^{-22} \bar{n}_e R^2 a q_\psi^{0.8}$. In JET neither R nor a have been varied significantly. Disruptive instabilities occur in JET if the ratio of mean electron density to mean current density exceeds a critical value.

The engineering performance of the machine has fully lived up to expectations. The plasma is hotter than expected (Bickerton 1982); however, densities and $\langle n\tau_E \rangle$ products are down on expectation. The principal reason is the higher than expected value of Z_{eff} due to the heavy contamination with impurities. Various methods to reduce the contamination will be tried, including pulse discharge cleaning, neon puffing, use of different aperture and gas-puffing scenarios etc. In the longer term it may prove necessary to line the whole of the inside of the torus with a low Z material such as carbon. A step in this direction will be taken at the end of 1984 by lining the small major radius side of the torus to a height of ± 1m with graphite tiles.

ACKNOWLEDGEMENTS

The results described were obtained by the efforts of a large team led by P H Rebut. Those who obtained and interpreted the main physics data include:-

D Bartlett, K Behringer, R Behrisch, M Brusati, D Campbell, P Carolan, J Christiansen, J G Cordey, S Corti, A Costley, M Gadeberg, A Gibson, R D Gill, B J Green, N Hawkes, A Hubbard, M Huguet, B de Kock, H Krause, F Mast, G McCracken, P Morgan, P Nielsen, P Noll, N J Peacock, F C Schueller, D Summers, A Tanga, P Thomas, G Tonetti.

REFERENCES

Rebut P H and Green B J — Plasma Physics and Controlled Fusion, 1A, 1, 1984

Hawryluk R J et al — Proceedings of Conference on Heating in Toroidal Geometry Rome, 1984

Bickerton R J — Physica Scripta, T2.2, 347, 1982

TABLE i

JET PARAMETERS

		Design Values	Used in data reported here
Plasma mean major radius	R_o(m)	2.96	$\sim$ 3.0
Maximum horizontal plasma radius	a(m)	1.25	$\leqslant$ 1.12
Maximum vertical plasma radius	b(m)	2.10	$\leqslant$ 1.90
Toroidal field strength at $R = R_o$	B_ϕ(T)	3.45	$\leqslant$ 2.6
Plasma current circular plasmas q(a) = 2.8	I_p(MA)	2.8	3.0 ($\frac{b}{a}$ = 1.25 q_ψ = 2.65)
Plasma current D-shaped plasma q(a) = 6.0	I_p(MA)	4.8	3.3 ($\frac{b}{a}$ = 1.6 q_ψ = 4.3)

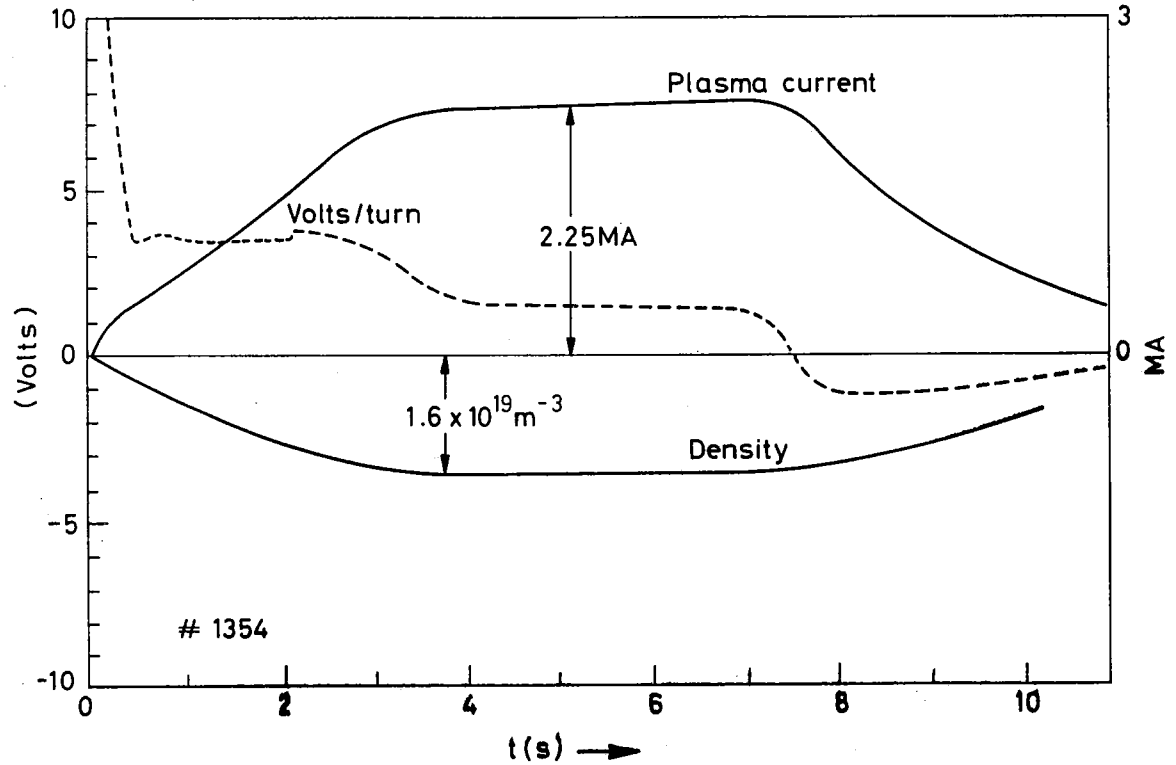

Fig. 1 Current, loop voltage and plasma density for discharge with $^{b}/_{a}$ = 1.2.

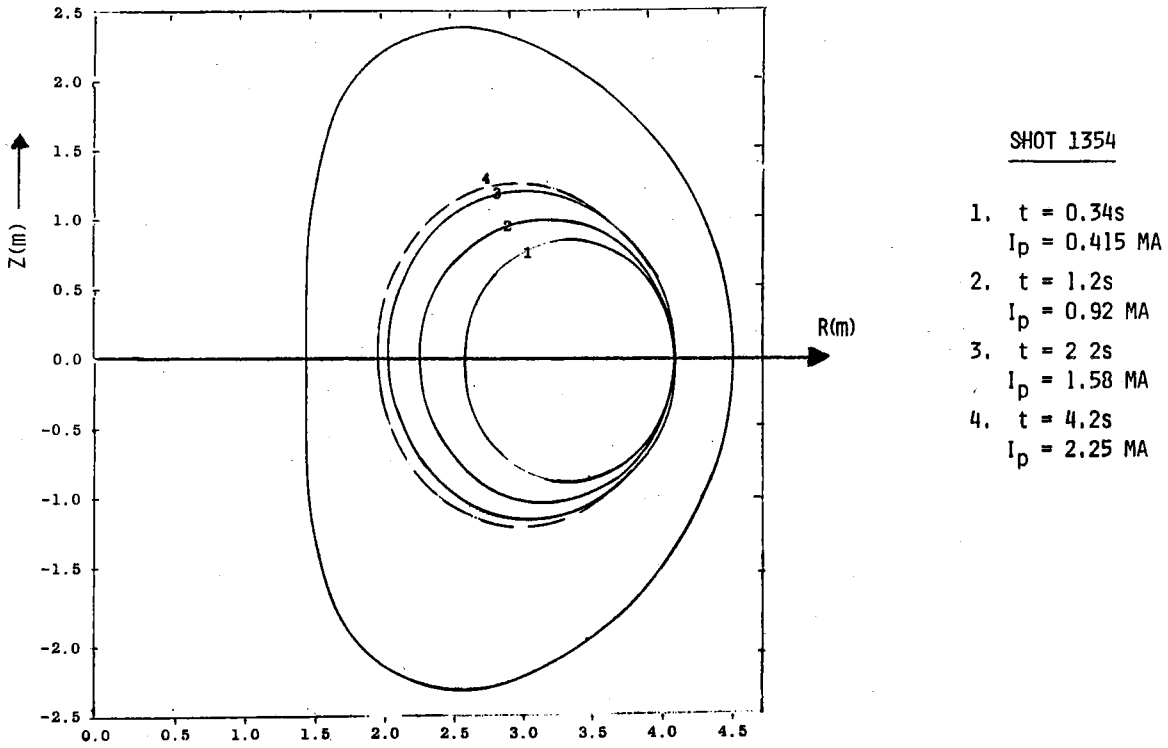

Fig. 2 Evolution of plasma boundary with time during current rise phase.

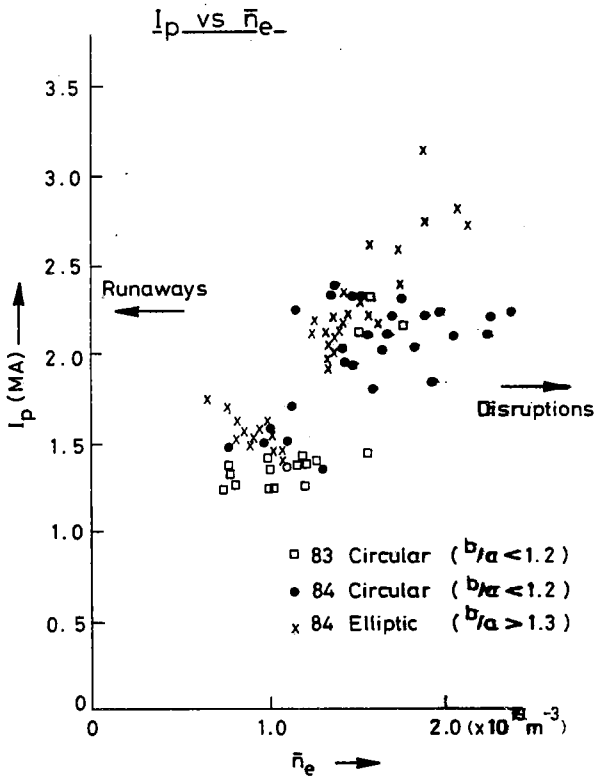

Fig.3 Flat-top values of plasma current (I_p) versus line average electron density ($\bar{n}_e$).

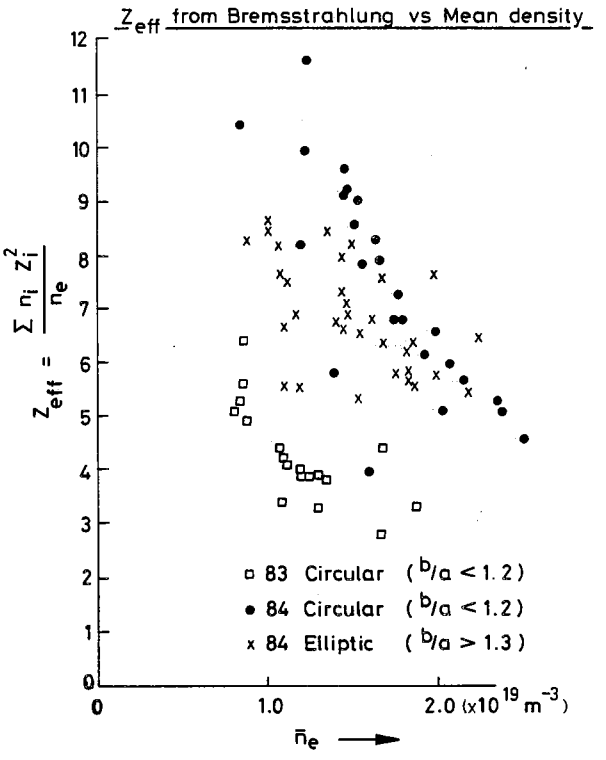

Fig.4 Flat-top values of Z_{eff} from visible bremsstrahlung versus line average electron density ($\bar{n}_e$).

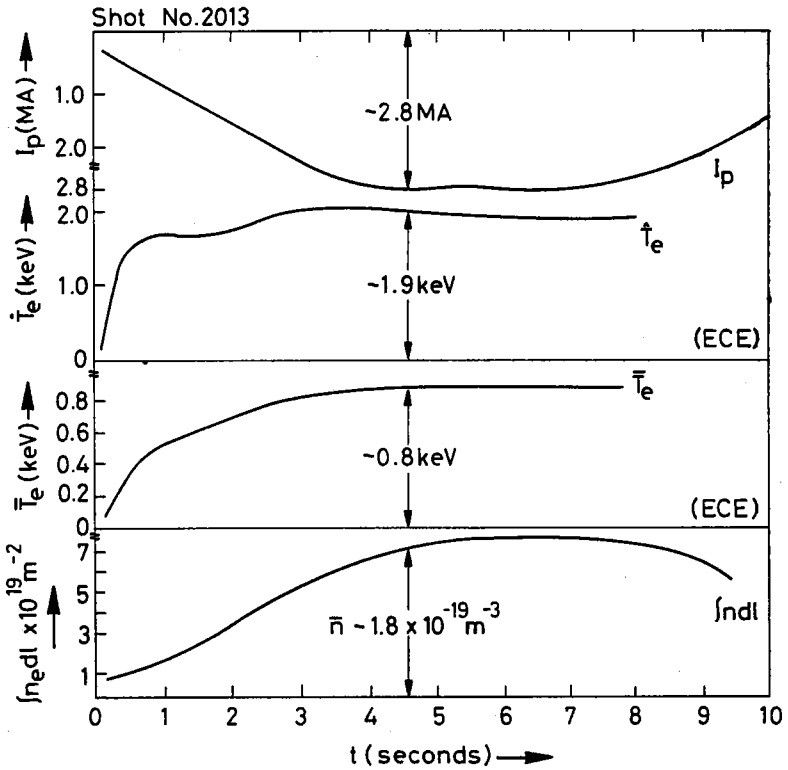

Fig.5 Plasma current (I_p), central electron temperature (T_e), area weighted average electron temperature ($\bar{T}_e$) and line integral of density ($\int nd\ell$) versus time. Shot 2013.

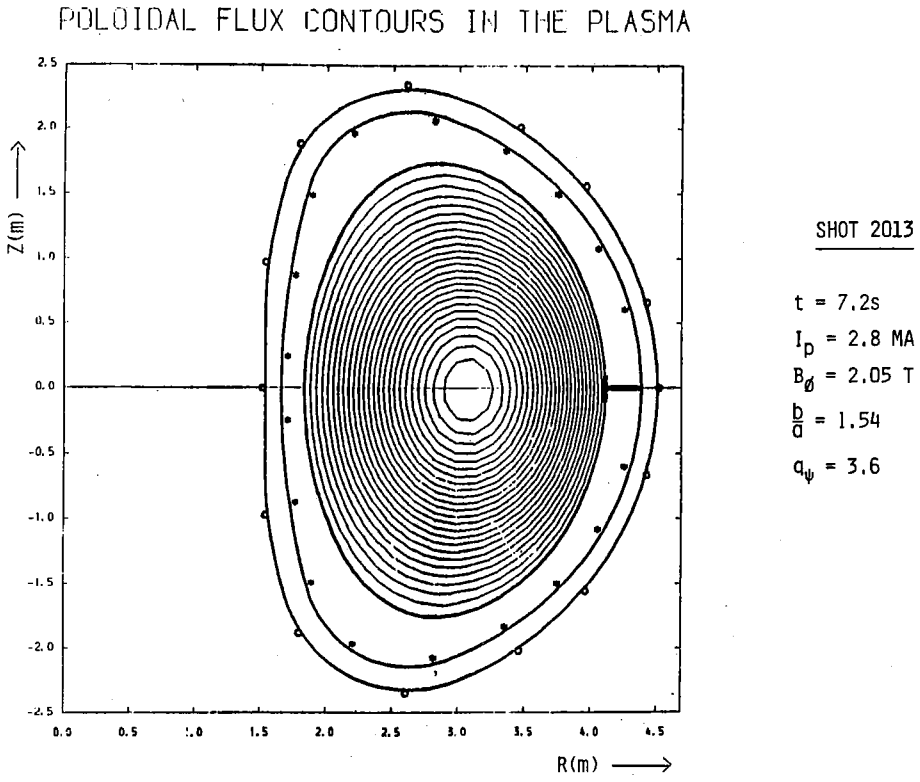

Fig.6 Poloidal flux contours in Shot 2012 at t = 7.2s, $^b/_a$ = 1.54, q_ψ = 3.6.

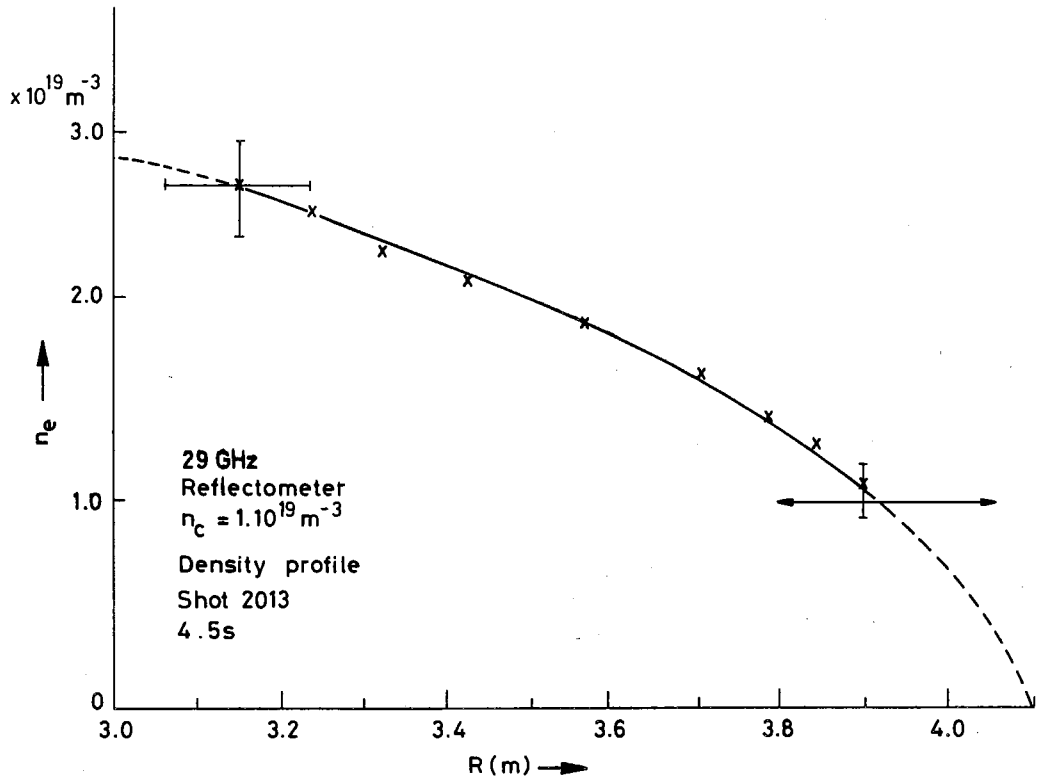

Fig. 7 Density profile, Shot 2013. Constructed at t = 4.5 s from earlier motion of critical layer measured by reflectometer.

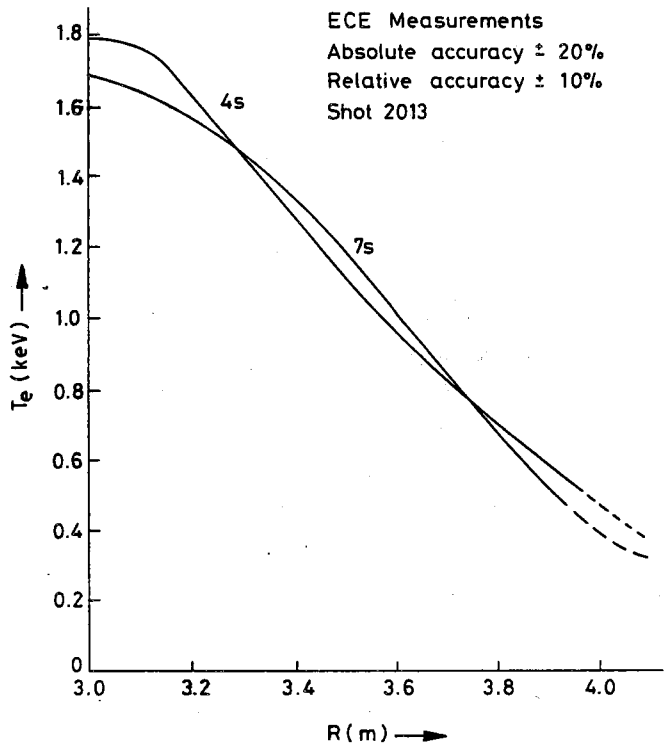

Fig. 8 Electron temperature profiles from cyclotron emission at beginning and end of current flat-top. Shot 2013.

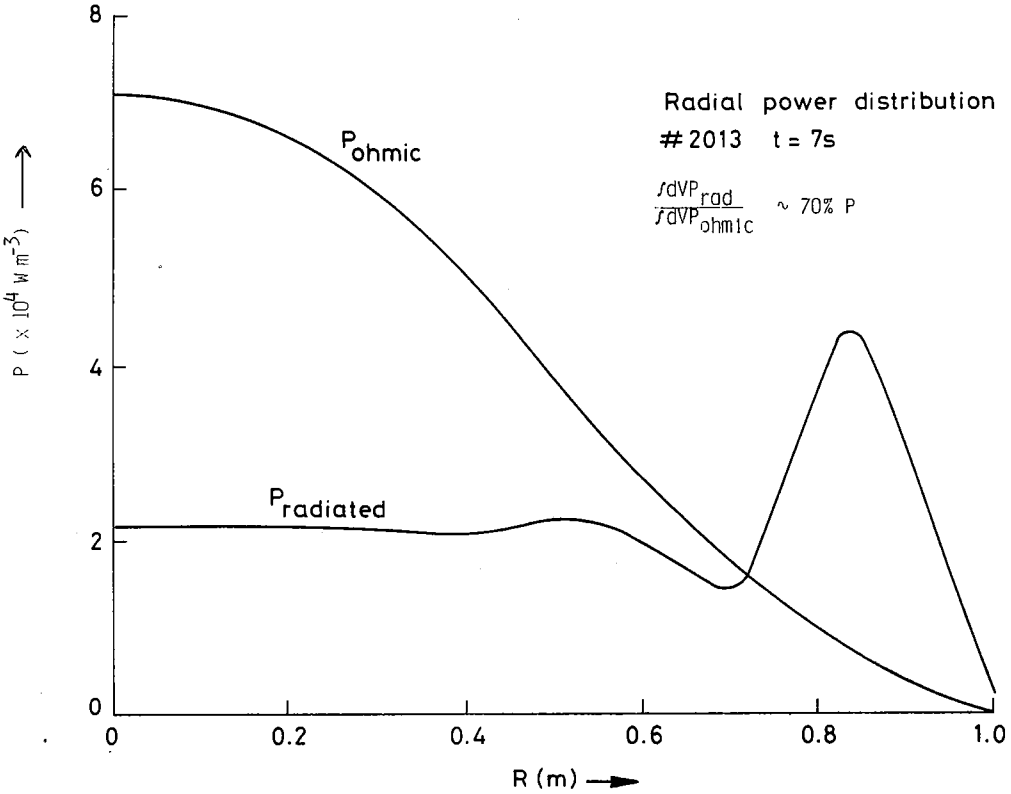

Fig.9 Radial distribution of ohmic input and radiated power. t = 7s. Shot 2013.

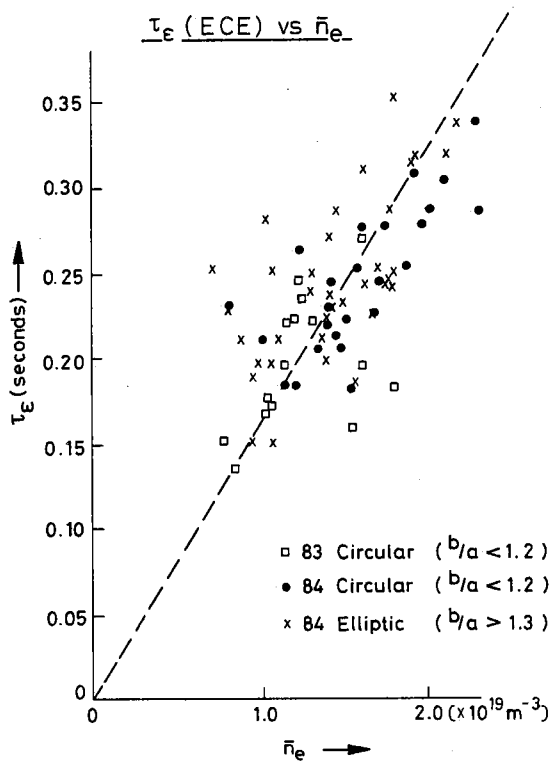

Fig.10 Global energy confinement time τ_ε versus line-average electron density $\bar{n}_e$.

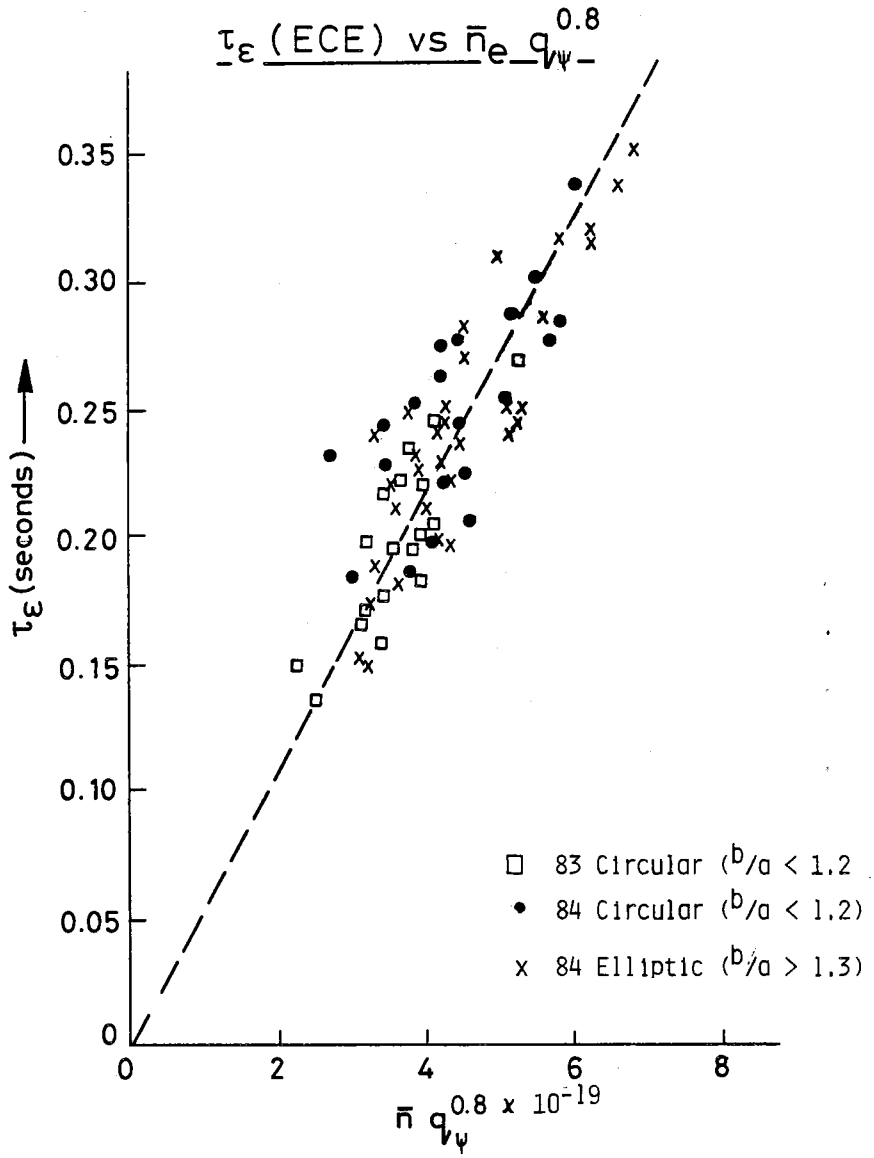

Fig. 11 Global energy confinement time versus $\bar{n}_e\, q_\psi^{0.8}$.